International Journal of Aquatic Science
ISSN: 2008-8019
Vol 12, Issue 03, 2021

# Optimal Model Order Reduction Based On $H_2$-Norm With Krylov Subspace Algorithm For SISO System

Sudhahar S[1], Ganesh Babu C[2], Sharmila D[3]

[1] *Department of EIE, Bannari Amman Institute of Technology, Sathyamangalam, Erode, Tamilnadu, India*

[2] *Department of ECE, KPR Institute of Engineering and Technology, Arasur, Coimbatore, Tamilnadu, India.*

*Email: [1]sudhahars@bitssathy.ac.in, [2]ganeshbabuc@bitssathy.ac.in, [3]sharmiramesh@rediffmail.com*

***Abstract. This article presents a $H_2$-norm optimal model technique for creating a reduced order model (ROM) / model order reduction (MOR) for the linear time-invariant (LTI) SISO stable system. The computational shortcut that results in models with lower-order frequency and time responses which are less similar to the original, The $H_2$-norm optimum model order decrease of the SISO model created which is based on the Gramian matrices and Krylov subspace algorithm. The Grampian matrix, which is derived from the controllability and observability matrices, the effectiveness of the projected algorithm is established by the benchmark SISO system. The efficiency is depends upon the preservation of dynamic characteristics of the original system and it is evaluated through the Root Mean Square Error (RMSE), frequency and time domain specifications.***

***Keywords: ROM / MOR, $H_2$-norm, Krylov subspace, RMSE, Time and Frequency Domain Specifications.***

## 1. INTRODUCTİON

For engineering processes, a system of large-scale differential equations is often used to describe the complex physical systems that appear. The role of simulations has increased greatly in the electronics and aerospace industries as a result of increased computerization and the mechanization of the design process. On the other hand, models that are proven to be reliable are accompanied by an increase in variables, which makes simulations longer and more expensive. Therefore, model reduction is required. The goal is to have the dynamic characteristics of the model approach accuracy as closely as possible, but to have as few variables involved in the model as possible. To express it another way, with respect to keep input and output characteristic of the model being close to what it was as possible, while also reducing the state variable count. An additional reward be alive the preservation of additional properties like stability, passivity, and so on. This study to reorder the system's components so that it could be fully controllable and observable, Direct simulation of these differential equations is generally not recommended because of a computational burden that is unacceptably high. A powerful design and control method for large-scale systems that can help significantly re-

duce simulation computational costs is known as model order reduction (MOR) [1]. For decades, MOR has been the focus of many investigations. a variety of clever MOR techniques have been utilized to deal with the continuous systems [2]. In the majority of operations, analytical representation used to designate physical occurrences are described by partial differential equations, it is also possible to approximate these complex equations using the linear systems. Discrete systems that implement the Crank–Nicolson scheme are generated [3]. Several balanced truncation (BT) techniques have been developed for discrete systems [4]. The projections, like Krylov subspace methods and orthogonal polynomial techniques, have also been implemented [5] and H∞ optimal methods in [6].

This approach to MOR of linear systems, which is called Chebyshev established, is described as being constructed on Chebyshev rational polynomials [7]. To build sets of lower-order models, estimates of the moments matching are proposed, and those estimations are utilized to build the reduced-order models. [8].

In this paper, the double-sided case of the frequency-weighted H2-optimal MOR problem within the projection framework is considered. The main motivation for seeking a projection-based solution is to avoid nonlinear optimization and benefit from the efficient Sylvester equation solver, particularly formulated for the projection based H2-optimal MOR algorithms. The exact satisfaction of the optimality conditions is inherently not possible within the projection framework. However, the optimality conditions can be nearly satisfied, and the deviation in the satisfaction of the optimality condition decays as the order of ROM grows. The conditions for exact satisfaction of the optimality conditions are also discussed. In addition, a projection-based iterative algorithm is proposed that solves the Sylvester equations in each iteration to construct the required ROM. Near first-order optimality conditions are found for the double-sided frequency-weightedH2-optimal MOR problem when convergence occurs. The efficacy of the projected algorithm is highlighted by dint of considering the benchmark numerical case.

*Preliminaries*

In the following, important preliminaries on LTI systems are summarized.

*3.1 State Space Models*

A general state space depiction of a linear time-invariant (LTI) model is given by $\begin{cases} \dot{x}(t) = A\,x(t) + B\,u(t) \\ y(t) = C\,x(t) + D\,u(t) \end{cases}$ with $A \in \Re^{NXN}$, $B \in \Re^{NXm}$, $C \in \Re^{pXN}$, and $D \in \Re^{pXm}$ (1)

Let us denote a n[th]-order stable linear time-invariant model by m inputs and p outputs as H(s), which is represented such as $H(s) = C*(sI - A)^{-1} * B + D$ (2)

Let us denote r[th]-order approximation about H(s) as $\tilde{H}(s)$, which is transcribed as $\tilde{H}(s) = \tilde{C} * \left(sI - \tilde{A}\right)^{-1} * \tilde{B} + D$ with $\tilde{A} \in \Re^{rXr}$, $\tilde{B} \in \Re^{rXm}$, $\tilde{C} \in \Re^{pXr}$, and $r \ll n$.(3)

In projection based MOR, the state space matrices $\tilde{A}$, $\tilde{B}$ and $\tilde{C}$ are computed by $\tilde{A} = \tilde{W}^T * A * V$, $\tilde{B} = \tilde{W}^T * B$ and $\tilde{C} = C * \tilde{V}$ (4)

The controllable and observable gramians of the realization (Aw, Bw, Cw) as Pw and Q respectively, which solve the following Lyapunov equations

$A_w P_w + P_w A_w^T + B_w B_w^T = 0$ (5)

$A_w^T Q_w + Q_w A_w + C_w^T C_w = 0$ (6)

The local optimum $\tilde{H}(s)$ of $\|E_w(s)\|_{H2}^2$ satisfies the following first-order optimality conditions

$\frac{\partial}{\partial \tilde{A}}\|E_w(s)\|_{H2}^2 = 0$ which implies $\bar{X} + X = 0$ (7)

$\frac{\partial}{\partial \tilde{B}}\|E_w(s)\|_{H2}^2 = 0$, which implies $\bar{Y}D_i D_i^T + Y = 0$ (8)

$\frac{\partial}{\partial \tilde{C}}\|E_w(s)\|_{H2}^2 = 0$, which implies $D_o^T D_o \bar{Z} + Z = 0$ (9)

With $\bar{X} = Q_{12}^T P_{12} + \tilde{Q}^T \tilde{P}$, $\bar{Y} = Q_{12}^T B + \tilde{Q}^T \tilde{B}$, $\bar{Z} = C P_{12} - \tilde{C} \tilde{P}$, $X = Q_{23} P_{23}^T + Q_{24} P_{24}^T$

$Y = \left(Q_{12}^T P_{12} + \tilde{Q} P_{23} + Q_{23} P_i + Q_{24} P_{34}^T\right) C_i^T + Q_{23} B_i D_i^T$

$Z = -B_o^T \left(Q_{14}^T P_{12} + Q_{24}^T \tilde{P} + Q_{34}^T P_{23}^T + Q_o P_{24}^T\right) + D_o^T C_o P_{24}^T$

*3.2. Frequency-weighted Tangential Interpolation*

The aim is to construct a ROM that should be satisfied by the following conditions

$\frac{\partial}{\partial \tilde{B}}\|W_o(s) E(s)\|_{H2}^2 = 2\left(Q_{12}^T B + \tilde{Q}^T \tilde{B}\right) = 0$ (10)

$\frac{\partial}{\partial \tilde{C}}\|E(s) W_i(s)\|_{H2}^2 = 2\left(C P_{12} - \tilde{C} \tilde{P}\right) = 0$ (11)

$\tilde{H}(s) = \sum_{i=1}^{r} \frac{\tilde{l}_i * \tilde{r}_i^T}{s - \tilde{\lambda}_i} + D$

$F[H(s)] = C_f * (sI - A_f)^{-1} * B_f$ and $G[H(s)] = C_g * (sI - A_g)^{-1} * B_g$

$A_f = \begin{bmatrix} A & BC_i \\ 0 & A_i \end{bmatrix}$ and $A_g = \begin{bmatrix} A & 0 \\ B_0 C & A_0 \end{bmatrix}$ (12)

$B_f = \begin{bmatrix} P_{13} C_i^T + B D_i D_i^T \\ P_i C_i^T + B_i D_i^T \end{bmatrix}$ and $B_g = \begin{bmatrix} B \\ B_o D \end{bmatrix}$ (13)

$C_f = \begin{bmatrix} C^T \\ C_i^T D_i^T \end{bmatrix}^T$ and $C_g = \begin{bmatrix} Q_{14} B_o + C^T D^T D_0 \\ Q_o B_o + C_o^T D_o \end{bmatrix}^T$ (14)

The conditions (10) and (11) are satisfied when the following tangential interpolation conditions are satisfied.

$F\left[H\left(-\tilde{\lambda}_i\right)\right]\tilde{r}_i = \tilde{F}\left[\tilde{H}\left(-\tilde{\lambda}_i\right)\right]\tilde{r}_i$ (15)

$\tilde{l}_i^T G\left[H\left(-\tilde{\lambda}_i\right)\right] = \tilde{l}_i^T \tilde{G}\left[\tilde{H}\left(-\tilde{\lambda}_i\right)\right]$ (16)

The poles $\tilde{\lambda}_i$ and residues $\left(\tilde{l}_i, \tilde{r}_i\right)$ of $\tilde{H}(s)$ are not known apriori. Thus the interpolation points and tangential directions are initialized arbitrarily, and after every iteration, the interpolation points $\sigma_i$ are updated as $-\tilde{\lambda}_i$ , and the tangential directions $(c_i, b_i)$ are updated as the residue $\left(\tilde{l}_i, \tilde{r}_i\right)$. The rational Krylov subspaces that seek to satisfy (15) and (16) are obtained.

*3.3 Conditions for Exact Satisfaction of the Optimality Conditions*

By expanding the Lyapunov equations (4) and (5) according to the structure of (Aw, Bw, Cw) in (3), it can be noted that P solve the following Sylvester equations

$\tilde{A} P_{23} + P_{23} A_i^T + \tilde{B}\left(C_i P_i + D_i B_i^T\right) = 0$ (17)

$\tilde{A} \tilde{P} + \tilde{P} \tilde{A}^T + \tilde{B} C_i P_{23}^T + P_{23} C_i^T \tilde{B}^T + \tilde{B} D_i D_i^T \tilde{B}^T = 0$ (18)

$$A P_{12} + P_{12}\ \widetilde{A}^T + B C_i\ P_{23}^T + P_{13} C_i^T \widetilde{B}^T + B D_i\ D_i^T\ \widetilde{B}^T = 0 \quad (19)$$

$$\widetilde{A}^T Q_{24} + Q_{24} A_o - \widetilde{C}^T \left(B_o^T Q_0 + D_o^T C_o\right) = 0 \quad (20)$$

$$\widetilde{A}^T * \widetilde{Q} + \widetilde{Q} * \widetilde{A} - \widetilde{C}^T * B_o^T * Q_{24}^T - Q_{24} * B_0 * \widetilde{C} + \widetilde{C}^T * D_o^T * D_o * \widetilde{C} = 0 \quad (21)$$

$$A^T Q_{12} + Q_{12} \widetilde{A} + C^T B_o^T Q_{24}^T - Q_{14} B_0 \widetilde{C} - C^T D_o^T D_o \widetilde{C} = 0 \quad (22)$$

The order of the ROM increases, then $\|W_o(s) E(s)\|_{H2}^2$ decreases. Consequently $\hat{Q}$ and $\hat{P}$ approaches Q and P respectively. The P and Q solved for the Lyapunov equations. The residuals $R_1$ and $R_2$ approaches zero.

The main steps to obtain the ROM, here's how the process works:

Step 1: Construct the state space matrices (A, B, C and D) from the original system transfer function identification of state space matrices (A, B, C and D) Matrices from the original state variable system.

Step 2: Calculate the initial system's input and output weights

Step 3: Initial values given to the ROM matrices $\left(\widetilde{A}, \widetilde{B}, \widetilde{C}\right)$

Step 4: Compute P and Q matrices

Step 5: Fix the projection length

Step 6: Compute the projection v, w from P and Q matrices

Step 7: Find the decomposed matrices $\left(\widetilde{V}, \widetilde{W}\right)$

Step 8: Determine the ROM state space matrices $\left(\widetilde{A}, \widetilde{B}, \widetilde{C}\right)$

## *4. The Quality of Model Order Reduction*

The dimension of the model reduction inaccuracy may be represented by the norm of the difference between G and the ROM Gr. This is possible through appraise the model reduction error using a scalar $\|G - G_r\|$. The established ROMs should be able to closer to the $H_2$ norm of the unique system. The $H_2$ norm of compound appreciated function G(s) is well-defined as

$$\|G(s)\|_{H2} = \sqrt{\frac{1}{2\pi} \int_{-\pi}^{\pi} \left|G\left(e^{j\omega}\right)\right|^2 d\omega} \quad (23)$$

The Root Mean Square Error (RMSE) = $J_{RMSE} = \sqrt{\dfrac{\sum_{i=1}^{N} \|y(i) - \hat{y}(i)\|^2}{N}}$ (24)

## *5. Simulations*

In this part, the projected method in reduced order model order reduction in terms of a higher-order system.

### *5.1 Illustrative Example*

Consider a $10^{th}$ order system with the following transfer function realization. This system models are reduced in different order, which is below the system order are given in Table 1. Fig. 1 and Fig. 2 depict the step output and frequency output of the original system and the ROM respectively.

\

| Order of ROM | Transfer Function of ROM |
|---|---|
| 1 | $\frac{0.1917}{s+0.1168}$ |
| 2 | $\frac{0.0496}{s^2+0.1879s+0.0302}$ |
| 3 | $\frac{0.0201}{s^3+0.3193s^2+0.0933s+0.0123}$ |
| 4 | $\frac{0.0098}{s^4+0.416s^3+0.2138s^2+0.0429s+0.006}$ |
| 5 | $\frac{0.0067}{s^5+0.6753s^4+0.4139s^3+0.1452s^2+0.0316s+0.0041}$ |
| 6 | $\frac{0.0177}{s^6+2.9552s^5+1.9332s^4+1.1497s^3+0.3842s^2+0.0849s+0.0108}$ |

$$H(s)=\frac{\left(\begin{array}{l}s^9+59s^8+1657.9s^7+28640.7s^6+334474.5s^5+2742122.4s^4\\+15867513.2s^3+62854022s^2+155453416.4s+182004673.4\end{array}\right)}{\left(\begin{array}{l}s^{10}+49.5s^9+1169s^8+17109s^7+171437.4s^6+122711s^4+6376179s^4\\+24002493s^3+64135934s^2+114485916.5s+110910010\end{array}\right)}$$

**Table: 1, Reduced Order Models**

## 2. RESULTS AND DISCUSSION

Table 2 displays the model performance comparison for different order systems. The model of the system increases the RMSE and H2-norm value is also increased. The RMSE characteristics of the different ROM with respect to original system is shown in Fig. 3. It is observed that first order ROM gives like a decay exponential curve. When the order of the system is increased, the characteristics of the system closer to the original system are apparent. The time output appearances of the systems is shown in Fig. 1. It is observed, here also the first order system reaches the steady state without damping and remaining systems are reaches the steady state with damping. Fig. 2 represents the Bode plot of the different order ROMs. It is observed that the original system, first order ROM and second order ROM are stable. The unity feedback closed loop stability for the ROM is shown in Fig. 4. From the Nyquist plot, it is observed that original, first and second order reduced models are having the closed loop stability and remaining ROMs are unstable. The second order model produces the mimic results to the original system in terms of stability. While the sixth order model performs better, it is unstable.

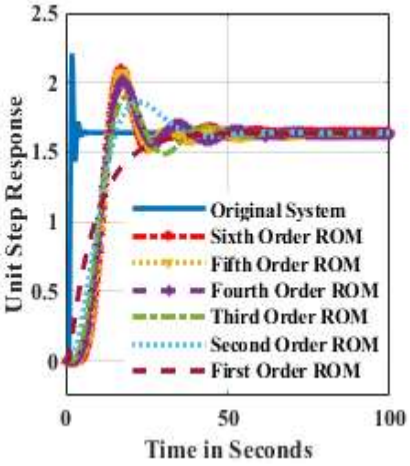


Fig. 1 Time Response

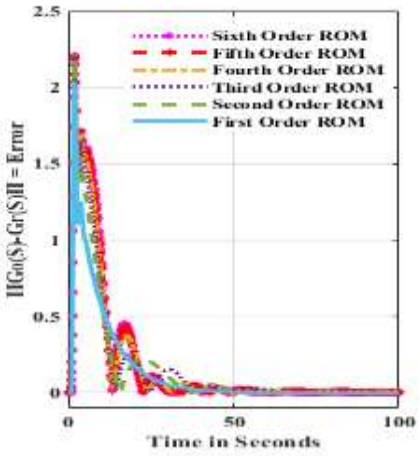


Fig. 3 Error Analysis

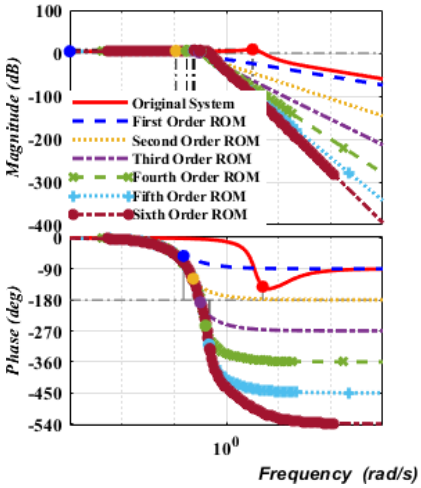


Fig. 2 Frequency Response

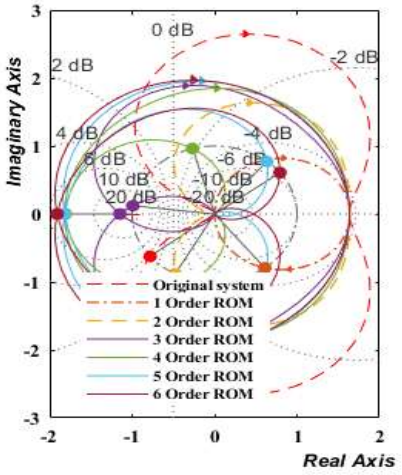


Fig. 4 Nyquist Stability Plot

Table: 2, Reduced Order Models

| Order of ROM | RMSE | BFR in % | $H_2$ - Norm |
|---|---|---|---|
| 1 | 0.426689715 | 89.59 | 0.3966 |
| 2 | 0.481920171 | 93.31 | 0.4656 |
| 3 | 0.506597532 | 95.23 | 0.5476 |
| 4 | 0.525094762 | 96.29 | 0.6272 |
| 5 | 0.538437403 | 96.5 | 0.6871 |
| 6 | 0.541855594 | 96.62 | 0.7064 |

## 3. CONCLUSION

In this article the $10^{th}$ order model is utilized to prove the efficiency of the proposed MOR method. The Krylov subspace algorithm is used for projection in state space and utilizing the H2-norm with Gramian matrices and Lyapunov equations. The second order model produce the mimic results to the original system in terms of stability. The stability of the system analyzed through the Bode plot and Nyquist plot. The sixth order model gives the better perfor-

mance than the second order reduced model, due to lack of preservation stability the model is not taken for further analysis. Reduced-order models are more computationally simple than procedures described in previous research, which also results in reduced-order models that have a similar frequency and time response. The efficiency is depends upon the preservation of dynamic characteristics of the original system and it is evaluated through the Root Mean Square Error (RMSE), frequency and time domain specifications.

## 4. REFERENCES

[1]. Semeraro, O., Bagheri, S., Brandt, L., & Henningson, S. D. Feedback control of three-dimensional optimal disturbances using reduced-order models. Journal of Fluid Mechanics, 677, pp.63-102 (2011).
[2]. Jiang, L. Y., & Chen, H. B. (2011). Time domain model order reduction of general orthogonal polynomials for linear input-output systems. IEEE Transactions on Automatic Control, 57(2), pp.330-343 (2011).
[3]. Chahlaoui, Y., & Van Dooren, P. A collection of benchmark examples for model reduction of linear time invariant dynamical systems, working note 2002-2 (2002).
[4]. Kotsalis, G., & Rantzer, A. (2010). Balanced truncation for discrete time Markov jump linear systems. IEEE Transactions on Automatic Control, 55(11), pp.2606-2611 (2010).
[5]. Zhang, H. L., Yang, H. W., Shen, C., & Li, C. R. A krylov subspace method for large-scale second-order cone linear complementarity problem. SIAM Journal on Scientific Computing, 37(4), pp.A2046-A2075 (2015).
[6]. Tong, D., Zhou, W., Gao, Y., Ji, C., & Su, H. H∞ model reduction for port-controlled Hamiltonian systems. Applied Mathematical Modelling, 37(5), pp.2727-2736 (2013).
[7]. Soloklo, N. H., & Farsangi, M. M. Chebyshev rational functions approximation for model order reduction using harmony search. Scientia Iranica, 20(3), pp.771-777 (2013).
[8]. Scarciotti, G., & Astolfi, A. Data-driven model reduction by moment matching for linear and nonlinear systems. Automatica, 79, pp.340-351 (2017).